

See discussions, stats, and author profiles for this publication at: <https://www.researchgate.net/publication/46007974>

Bioactive Polyelectrolyte Multilayers: Hyaluronic Acid Mediated B Lymphocyte Adhesion

ARTICLE *in* BIOMACROMOLECULES · SEPTEMBER 2010

Impact Factor: 5.75 · DOI: 10.1021/bm100570r · Source: PubMed

CITATIONS

24

READS

67

5 AUTHORS, INCLUDING:



Fernando Da Cruz Vasconcellos

University of Cambridge

17 PUBLICATIONS 254 CITATIONS

SEE PROFILE

Bioactive Polyelectrolyte Multilayers: Hyaluronic Acid Mediated B Lymphocyte Adhesion

Fernando C. Vasconcellos,[†] Albert J. Swiston,[‡] Marisa M. Beppu,[†] Robert E. Cohen,[§] and Michael F. Rubner^{*,‡}

Department of Thermofluidynamics, School of Chemical Engineering, State University of Campinas, UNICAMP, Campinas, São Paulo, Brazil, and Departments of Materials Science and Engineering and Chemical Engineering, Massachusetts Institute of Technology, MIT, Cambridge, Massachusetts 02139

Received May 26, 2010; Revised Manuscript Received July 19, 2010

A strategy was developed to produce thin, biopolymer-based polyelectrolyte multilayer films, based on hyaluronic acid and chitosan, that are able to effectively bind B lymphocytes. These films explore CD44–hyaluronate interactions and provide a method to make surface-bound B cell arrays without the need for nonselective covalent chemistry. The rational design of these films using solution deposition variables, such as ionic strength and pH, allows one to maximize and fine tune this binding efficiency *ex vivo*. This work suggests two important conditions for successfully attaching B cells to hyaluronate-containing polyelectrolyte multilayer films: (1) hyaluronic acid is required for the proposed CD44-mediated binding mechanism, and (2) hyaluronic acid deposition conditions that favor loops and tails, such as low pH and with added salt, result in more available CD44 binding ligands and higher cell binding efficiency. Chitosan-terminated films prepared without NaCl in the deposition solutions and hyaluronic acid-terminated films prepared with salt, both under pH 3.0 assembly conditions, presented a similar high lymphocyte binding efficiency. In the former case, however, the binding strength was weaker due to a significant electrostatic contribution to the binding. Bioactive polyelectrolyte multilayers for selective binding of lymphocytes hold great promise in fields ranging from cell-based biosensors to immune system engineering.

Introduction

Strategies for immobilizing nonadherent immune cells onto surfaces are of great interest for fundamental immunological studies, cell-based biosensors, and immune system engineering applications. Few immune cell immobilization methods have been described in the literature.^{1,2} Kim and co-workers presented a method to obtain B cell arrays using nonlithographic microscopic patterning of synthetic polymers, and utilizing specific antibodies or streptavidin–biotin interactions for B cell attachment.¹ This immobilization method was extended in a following work where patterned hydrogel microwells functionalized with antibodies were fabricated to immobilize T cells for sensitive detection of peptide analytes and monitoring of T and B lymphocyte interactions.²

B Lymphocytes are cells of the adaptive immune system that have evolved to identify pathogens very efficiently. They are, due to their sensing abilities, exceptional candidates for cell-based biosensors in applications such as diagnostics of infectious diseases and in immune system engineering applications where they can be used to home into diseased tissue.³ Previous results from our group have shown a particular application of biopolymer-based polyelectrolyte multilayers (PEMs), namely, the functionalization of B and T cells with cellular “backpacks”.⁴ The attachment of these backpacks involved a CD44-mediated interaction of the lymphocyte with hyaluronic acid (HA), which was presented as the top layer of the multilayer assembly.

This study describes biopolymer-based multilayer films that promote the adhesion of typically nonadherent B lymphocytes to surfaces. These PEMs were prepared by the layer-by-layer

(LbL) technique: a simple, versatile, and cost-effective method to create, modify, and functionalize a variety of surfaces.⁵ Weak polyelectrolyte biopolymers are great candidates for the preparation of PEMs due to their tunability through assembly conditions and their hydrophilic, nontoxic, bioactivity, biocompatible, and biodegradable properties.^{6–8} Chitosan (CHI) and HA are natural polysaccharides that display these desirable properties. CHI, a polycation derived from the naturally occurring polymer chitin, has been used in tissue engineering, drug delivery, and antibacterial applications.⁹ HA, a naturally occurring high molecular weight polyanion, is also a ligand for CD44, a cell-surface receptor found on several types of immune system cells.¹⁰ Several studies have focused on how deposition variables such as salt¹¹ and pH¹² change PEM film morphology and biological characteristics for encapsulation^{13,14} or attachment of adherent cells.^{6,7,13–22} In contrast to these studies of adherent cells, to our knowledge, Swiston et al.⁴ have made the only report of using CHI/HA PEMs to bind nonadherent cells.

We report on how HA/CHI PEMs can be used to immobilize nonadherent B lymphocytes to a surface, using the versatile, conformal layer-by-layer coating process. Deposition parameters such as salt (0 or 100 mM), pH (3.0 or 5.0), and final polymer deposited (HA vs CHI) were systematically adjusted to optimize binding efficiency via CD44–HA interactions.

This work shows two important conditions for successfully attaching B cells to HA-containing PEM films. First, HA is required for the proposed CD44-mediated binding. Second, HA deposition conditions that favor loops and tails, such as low pH and with added salt, can result in more available CD44-binding ligands and, thus, greater B cell attachment. These two conditions emphasize that the most important factor affecting cell binding potential is the presentation and configuration of

* To whom correspondence should be addressed. E-mail: rubner@mit.edu.

[†] Department of Thermofluidynamics, UNICAMP.

[‡] Department of Materials Science and Engineering, MIT.

[§] Department of Chemical Engineering, MIT.

HA on a surface, conditions controllable in PEM film assembly by changing solution deposition conditions (such as salt and pH).

Experimental Section

Materials. Hyaluronic acid sodium salt (HA, from *Streptococcus equi* sp, MW $\approx 1.58 \times 10^6$ g/mol), chitosan (CHI, low molecular weight $\approx 5 \times 10^4$ g/mol, 75–85% deacetylated), alginate (ALG, in the form of alginic acid sodium salt, low molecular weight ≈ 12 – 19×10^4 g/mol), poly(diallyldimethylammonium chloride (PDAC, medium molecular weight, 20 wt % in water solution), poly(sodium 4-styrenesulfonate) (SPS, MW $\approx 7 \times 10^4$ g/mol), and fluorescein isothiocyanate-labeled poly(allylamine hydrochloride) (FITC-PAH) were purchased from Sigma-Aldrich (U.S.A.). All polyelectrolytes were used without further purification. Anionic, superparamagnetic nanoparticles (MNPs, Fe₃O₄ EMG 705, 13 nm diameter) were purchased from FerroTec (U.S.A.). RPMI-1640 cell culture media and streptomycin/penicillin (S/P, 5000 U.I./mL) were purchased from CellGro, Inc. (U.S.A.). Fetal calf serum (FCS) was purchased from Hyclone (U.S.A.). Hank's balanced salt solution (HBSS) was purchased from Gibco, Invitrogen (U.S.A.). The positive photoresist S-1813 and MF-319 developing solution were purchased from MicroChem. All chemicals were reagent grade and used without further purification. CH27 B lymphocytes were kindly provided by Prof. Irvine's lab in the Department of Materials Science and Engineering at MIT. Premium precleaned VWR glass slides and clean-room grade polished (100) silicon wafer slides were used as substrates. Milli-Q-grade water (Millipore) with a resistivity of 18.2 M Ω ·cm was used for all solutions.

VWR Glass and Si Wafer Substrate Preparation. Before use, VWR glass slides were sonicated for 15 min in a 3% detergent (Micro 90) aqueous solution followed by a 10 min wash in 1 M NaOH and two consecutive 5 min rinses in Milli-Q water. All samples were air-dried. Si wafers were cut to the desired sample size, wiped with ethanol, O₂ plasma cleaned, and air-dried before use.

Polyelectrolyte and Nanoparticle Solutions. PDAC and SPS solutions were prepared at 10^{-2} M (based on the repeat unit molecular weight) in 100 mM NaCl. CHI, HA, and ALG solutions were prepared by dissolving the respective polymer in water at concentrations of 1 mg/mL and gently stirring the solution overnight. The CHI solution was prepared with 100 mM glacial acetic acid (HOAc). HA, CHI, and ALG solutions were prepared both with and without 100 mM NaCl. The pH of all solutions was adjusted with 1 M HCl or NaOH solutions. MNP solutions were prepared at a concentration of 0.005% w/v at pH 4.0.

Polyelectrolyte Multilayer Assembly. The LbL technique was used to deposit the heterostructured polymer and nanoparticle films. The notation that is used for each bilayer of complementary polymers or nanoparticles is (Poly₁X/Poly₂Y)_n. Poly₁ and Poly₂ refer to the polymers or nanoparticles, X and Y refer to the solution pH, and *n* is the number of bilayers deposited. A half bilayer is represented when *n* = *x*.5, where *x* is any integer. A (PDAC4/SPS4)_{15.5} prelayer was deposited on all substrates using an automatic dipping procedure with a Zeiss HMS Series Programmable Slide Stainer. Clean glass or Si wafer slides were alternately immersed in PDAC (pH 4.0, 100 mM NaCl) and SPS (pH 4.0, 100 mM NaCl) solutions for 10 min, each followed by two consecutive Milli-Q water (pH \sim 5.7) rinse steps of 2 and 1 min, respectively. The (PDAC4/SPS4)_{15.5} layers provide a positively charged surface that promotes uniform deposition of HA/CHI multilayers. Samples were stored overnight at ambient conditions before performing B lymphocyte adhesion studies.

Lymphocyte Adhesive HA/CHI Region. HA/CHI bilayers were deposited with a StratoSequence VI spinning dipper running StratoSmart v6.2 software from nanoStrata Inc. (U.S.A.). HA and CHI polyelectrolyte deposition steps were performed without stirring for 10 min. The three consecutive rinse steps (2, 1, and 1 min) with pure Milli-Q water were performed while spinning the substrate within the solutions at a frequency of approximately 100 rpm.

CH27 B Lymphocyte Culture. CH27 B lymphocytes were cultured and passaged (1:10 every 3 days) in RPMI-1640 media containing 10% fetal calf serum (FCS), and 1% streptomycin/penicillin (P/S). Cell cultures were maintained at 37 °C and 5% CO₂. Adhesion experiments were performed with cell aliquots at 10^6 cells/mL. Cells were washed in HBSS three times prior to attachment.

B Lymphocyte Attachment to PEMs. B Lymphocyte suspensions (2 mL) were gently pipetted directly onto the prepared HA/CHI multilayered surfaces in Petri dishes. These dishes were placed on a vibratory platform (IKA Vibrax) inside an incubator. Samples were incubated for 15 min, followed by a gentle agitation for 15 min. This procedure was repeated twice (for a total time of 1 or 2 h) to promote cell adhesion. Immediately after the incubation/agitation steps, samples were gently washed in fresh HBSS to remove unbound cells, then placed in complete RPMI-1640 media and analyzed.

PEM Thickness and Roughness. Dry film thickness and rms roughness measurements were measured using a P-16+ stylus profilometer (KLA Tencor Corporation, U.S.A.) with the following parameters: 0.50 mg applied force, 200 Hz sampling rate, 50 μ m/sec scan speed, 131/0.0781 Å range/resolution.

UV–Visible Spectroscopy. Free HA carboxylic acid groups were stained by immersing the film in an alcian blue solution (0.001 M, pH 3.0) for 15 min. Slides were then rinsed extensively in pH 3.0 Milli-Q water twice for 2 min. Films were dried with N₂ and immediately analyzed in a Cary 5E UV–vis spectrophotometer. Alcian blue peaks were observed at 617 nm. Free CHI ammonium groups were stained by immersing the PEM in a rose bengal solution (0.001 M, pH 7.0) in RPMI media (with 25 mM HEPES, without FCS, phenol red, or S/P) for 15 min. The slides were then rinsed extensively in Milli-Q water twice for 2 min each. Films were dried with N₂ and absorbance was immediately measured. Peaks for rose bengal were observed at 567 nm. Films were also immersed overnight in Milli-Q water with the same pH as their respective build-up pH conditions (pH 3.0 and 7.0) and measured again. Measurements include absorption from multilayers on both sides of the substrate. The pH conditions for the dye experiments were chosen to produce the most reliable and reproducible staining effects for this multilayer system.

B Lymphocyte Binding Efficiency. Planar films and patterned film arrays with adhered CH27 B lymphocytes were analyzed with an Olympus IX-81 inverted optical microscope. At least seven images for each sample were analyzed and either the total number of cells attached per unit area (for planar films) or the percentage of patterned array sites occupied with a cell was determined.

PEM Film Patterned Arrays. The patterning method of McShane and co-workers^{23,24} and Swiston et al.⁴ was used to create patterned multilayer heterostructure assemblies. Briefly, this process uses a traditional lift-off photolithographic approach to pattern ultrathin polymer films. These assemblies were fabricated with a (MNP4/FITC-PAH3)_{9.5} region between the prelayer and cell adhesion regions. Deposition of the (MNP4/FITC-PAH3)_{9.5} region on the (PDAC4/SPS4)_{15.5} prelayer was performed by a Zeiss HMS static dipper. Two consecutive pH 3.0 Milli-Q water rinse steps were performed after each deposition step. After 9.5 bilayers were deposited, samples were allowed to dry in ambient conditions, and stored away from light. To build the cell adhesive region, CHI was deposited first on the negatively charged MNP surface. The same pH, NaCl, and top layer variations, as studied for planar films, were performed to evaluate B lymphocyte binding to these arrays.

Results

Multilayer Assembly. Given the weak polyelectrolyte nature of both HA and CHI, it is important to consider the solution pH values used during multilayer assembly. The pK_a of HA in salt free solution is about 2.9, whereas the pK_a of CHI is about 6.0 in 0.1 M acetic acid solution.^{25–28} Above pH 6.0, the solubility of CHI in water becomes problematic. Hence, we chose to focus on solution pH values of 3.0 and 5.0. To promote

Table 1. Thickness and Roughness Values of 3–3.5 Bilayer HA/CHI Films Deposited on a (PDAC4/SPS4)_{15.5} Prelayer^a

biopolymer film	salt condition (mM NaCl)	thickness (nm)	rms roughness (nm)	final polymer deposited
(HA3/CHI3) ₃	0	17	2	chitosan
(HA3/CHI3) _{3.5}	0	37	4	hyaluronic acid
(HA3/CHI3) ₃	100	27	2	chitosan
(HA3/CHI3) _{3.5}	100	42	3	hyaluronic acid
(HA5/CHI5) ₃	0	42	7	chitosan
(HA5/CHI5) _{3.5}	0	43	8	hyaluronic acid
(HA5/CHI5) ₃	100	39	5	chitosan
(HA5/CHI5) _{3.5}	100	49	10	hyaluronic acid

^a The average was obtained from seven measurements, each one performed on seven replicates.

uniform multilayer assembly, glass and silicon wafer substrates were precoated with a uniform charged multilayer thin film containing the strong polyelectrolytes PDAC and SPS. The (PDAC4/SPS4)_{15.5} precursor film used in this study had an approximate thickness of 57 nm and rms roughness of about 2 nm, as measured by profilometry. Biopolymer PEM deposition was initiated by the adsorption of HA on the positively charged PDAC surface followed by alternate depositions of CHI and HA. In addition to variations in solution pH (pH 3.0 vs 5.0), the ionic concentration of the deposition solutions was also varied (0 vs 100 mM NaCl). In general, film thickness increased in a nonlinear fashion with the number of deposition steps (see Supporting Information). These results corroborate the findings of Picart and co-workers,⁶ who attributed this exponential growth mechanism to CHI's ability to diffuse in and out of the entire HA/CHI film at each deposition step. These authors also reported that HA is a nondiffusing species in LbL assembly of PEMs. Recent detailed studies on the film build up of systems comparable to the HA/CHI films have also been reported by Porcel et al.^{29,30}

Table 1 presents thickness and roughness values for 3 and 3.5 bilayer HA/CHI PEMs deposited on the (PDAC4/SPS4)_{15.5}

precoating layers under the different assembly conditions examined. Compared to films assembled on the prelayers, it was observed that films assembled directly on glass required 10 or more bilayers to become uniform. Multilayer films with 3.0 and 3.5 bilayers have CHI and HA as the final deposited polymer, respectively. As expected,¹¹ the addition of 100 mM salt to the dipping solutions generally resulted in an increase in overall multilayer film thickness. In addition to charge screening effects, added salt can promote interdiffusion and mobility of oppositely charged polymers within a film,^{31,32} which leads to thicker films according to the diffusion-based film growth model.⁶ This trend was observed for all systems except for the multilayer assembled at pH 5.0 (three bilayer film) that was slightly less thick when salt was added compared to the salt-free deposition.

CH27 B Cell Binding. Figure 1 summarizes B lymphocyte binding trends on planar (HA/CHI) films prepared under the pH and salt conditions outlined above. Optical micrographs of B cells adhering to select PEM films can be found in Figure 2. For PEMs prepared at pH 3.0, the salt concentration and polymer deposited last modulates B lymphocyte binding over a relatively wide range. In contrast, multilayer films assembled at pH 5.0 exhibited overall lower binding efficiency that was less sensitive to the pH, salt, and final polymer deposited. High binding efficiencies were found with either HA (at 1850 ± 150 cells/mm²) or CHI (at 1840 ± 50 cells/mm²) terminated films assembled at pH 3.0. This means that even in the case that CHI is deposited last, there is a sufficient presentation of accessible binding ligands available on the surface. The two least efficient cell-binding films, (HA3/CHI3)_{3.5} deposited without salt and (HA3/CHI3)₃ deposited with 100 mM NaCl, bound cells at 1200 ± 200 cells/mm² and 770 ± 25 cells/mm², respectively. These results demonstrate that significant variations in B cell binding to CHI/HA multilayers can be realized through changes in easily controlled multilayer processing parameters (such as pH, salt, and final polymer deposited).

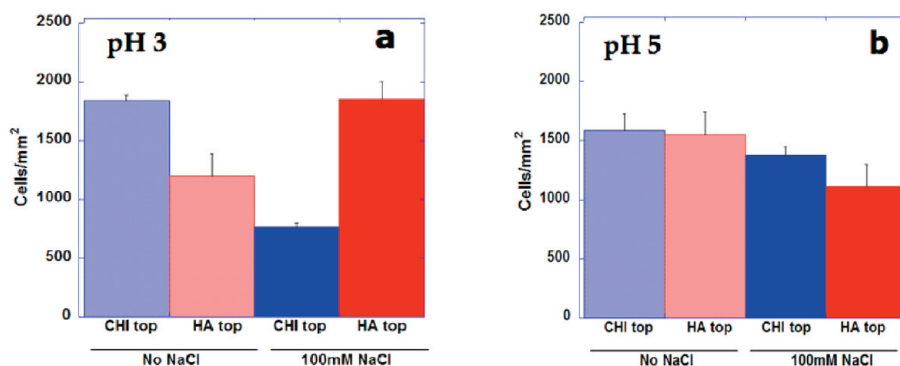


Figure 1. B Lymphocyte binding to (a) (PDAC4/SPS4)_{15.5}-(HA3/CHI3)_{3,x} and (b) (PDAC4/SPS4)_{15.5}-(HA5/CHI5)_{3,x} films, for $x = 0$ or 5. Error bars correspond to the standard error of the sample mean for seven independent measurements on seven replicates.

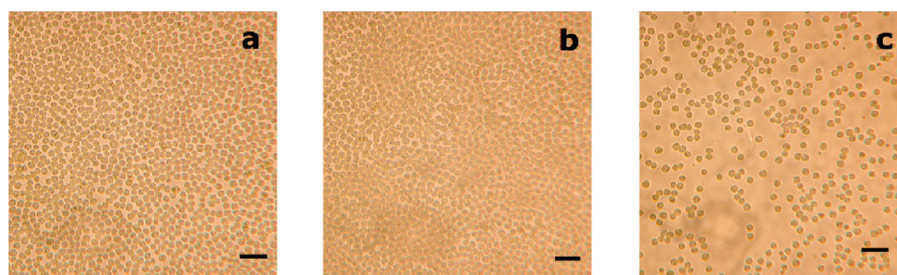


Figure 2. Optical micrographs of B cells adhered to (a) (PDAC4/SPS4)_{15.5}-(HA3/CHI3)_{3.5} film made with 100 mM NaCl (the best lymphocyte binding PEM), (b) (PDAC4/SPS4)_{15.5}-(HA3/CHI3)₃ film made with no NaCl (the second best binding system), and (c) (PDAC4/SPS4)_{15.5}-(HA3/CHI3)₃ film made with 100 mM NaCl (least effective binding PEM). Scale bars = 50 μ m.

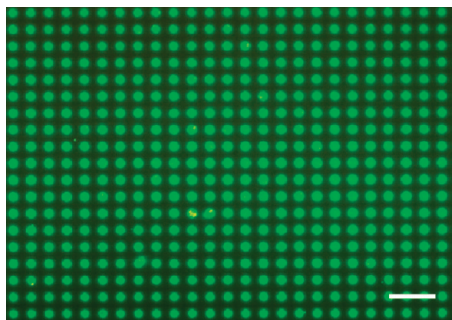


Figure 3. Fluorescent image of a $(\text{MNP4/FITC-PAH3})_{9.5}(\text{CHI3/HA3})_3$ built with 100 mM NaCl patterned slide. Scale bar = 50 μm .

Lymphocyte Binding to PEM Arrays. In addition to planar PEMs, patterned film arrays of 7 μm posts (Figure 3) were fabricated via a photolithographic lift-off technique.^{4,23,24} Experiments with patterned arrays were used to help quantify in a more controlled manner the number of cells adhered to a particular multilayer system. The compositions of these films were $(\text{MNP4/FITC-PAH3})_{9.5}(\text{CHI3/HA3})_x$ for $x = 3$ or 3.5. It should be noted that 3 bilayers refers to hyaluronic acid being deposited last and 3.5 refers to chitosan deposited last, which is reversed from the nonpatterned films discussed above. Both the (MNP4/FITC-PAH3) and the $(\text{CHI/HA})_x$ regions remain intact during the photoresist lift-off step and both maintain their functionality postfabrication. The (MNP4/FITC-PAH3) region was chosen for its usefulness in imaging and our experience with patterning these films.⁴

B Lymphocytes in 37 °C RPMI media were gently pipetted onto slides with patterned posts and incubated for 1 or 2 h with intermittent gentle agitation. The cell array was washed with Hank's balanced salt solution (HBSS) following cell seeding and incubation. Figure 4 presents typical examples of B lymphocytes adhered to arrays of HA- and CHI-terminated multilayers deposited with and without NaCl.

Figure 4 shows arrays with roughly the same occupancy ($\sim 55\%$), except for $(\text{CHI3/HA3})_3$ fabricated with 100 mM NaCl, for which $\sim 71\%$ of array sites were occupied (Figure 4b). For all multilayers tested, an even greater array occupation could be achieved by increasing the seeding time from 1 to 2 h, as seen in Figure 5a,b. Although well-ordered B lymphocyte arrays were generally observed, other arrangements were also seen: lymphocytes aggregated in interstitial spaces, more than one cell on a PEM array site, and empty sites. The interstitial space is a cationic PDAC-terminated surface. B cells seeded on a uniform $(\text{PDAC4/SPS4})_{15.5}$ surface showed an attachment density of approximately 310 cells/ mm^2 , which explains why we observe limited attachment on nonarray positions (see Figure 5c). Compared to the HA/CHI systems, the attachment density of cells on the PDAC/SPS prelayers is 60–83% lower.

From the above array experiments, different cell-attachment parameters were measured, including available sites occupied by B cells, the number of sites shared by two cells, and the number of cells adhered off array sites. These results are presented in Table 2.

Proceeding with the assumption that B cell binding to CHI/HA multilayers is facilitated by the previously established CD44 receptor interaction with HA chain segments,¹⁰ the above results point to specific assembly conditions that enrich the multilayer surface in accessible, cell binding HA segments. Two tests were utilized to confirm that HA is responsible for B-cell binding. First, HA was replaced in the multilayer with the very similar, non-cell-binding polysaccharide alginic acid (ALG). CHI/ALG multilayers with 3 and 3.5 bilayers were built under pH 3.0 conditions in the absence of NaCl. In this case, no B lymphocyte binding was observed with either CHI or ALG as the top layer. In fact, these multilayers are excellent blocking surfaces if one desires to prevent the binding of B cells to surfaces. This finding suggests that HA is critical to B lymphocyte binding mediated by CD44–HA interactions and that the positive charge of CHI alone is insufficient to provide efficient cell binding to the

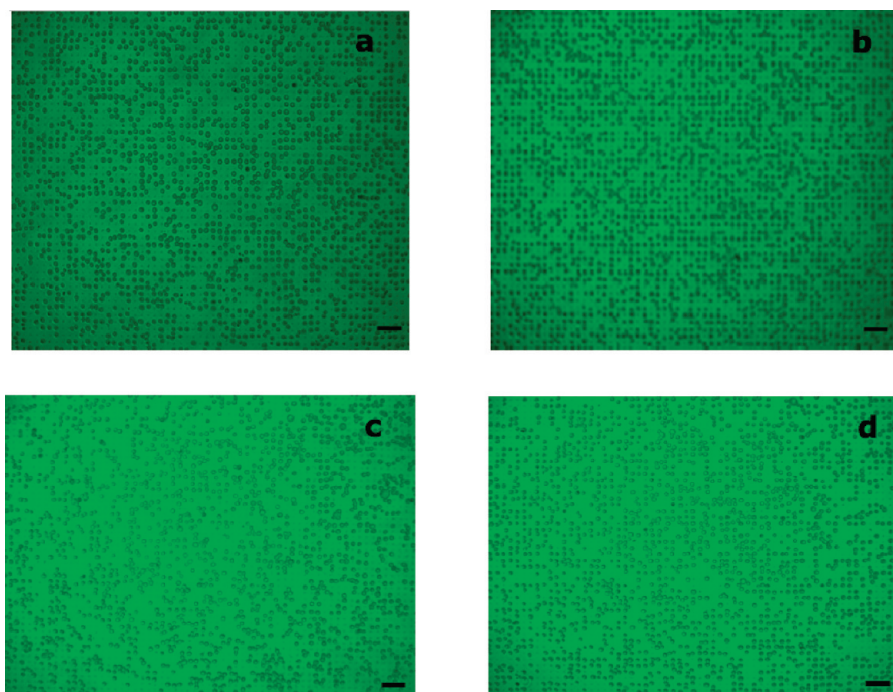


Figure 4. B Lymphocyte arrays on (a) $(\text{MNP4/FITC-PAH3})_{9.5}(\text{CHI3/HA3})_3$ ($\sim 57\%$ occupancy), (b) $(\text{MNP4/FITC-PAH3})_{9.5}(\text{CHI3/HA3})_3$ built with 100 mM NaCl ($\sim 71\%$ occupancy), (c) $(\text{MNP4/FITC-PAH3})_{9.5}(\text{CHI3/HA3})_{3.5}$ ($\sim 54\%$ occupancy), and (d) $(\text{MNP4/FITC-PAH3})_{9.5}(\text{CHI3/HA3})_{3.5}$ built with 100 mM NaCl ($\sim 56\%$ occupancy) after 1 h of agitation and incubation. Scale bars = 50 μm .

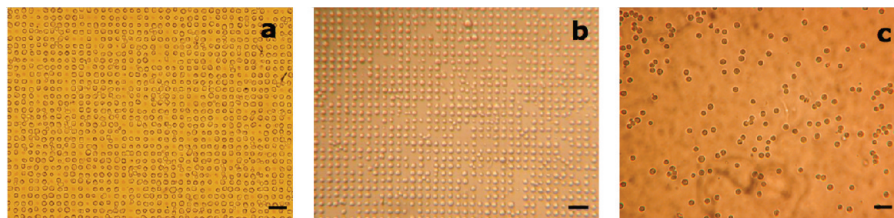


Figure 5. B Lymphocyte arrays after 2 h of agitation and incubation on (a) (MNP4/FITC-PAH3)_{9.5}-(CHI3/HA3)₃ built with 100 mM NaCl (~97% occupancy) and (b) (MNP4/FITC-PAH3)_{9.5}-(CHI3/HA3)_{3.5} (~90% occupancy). (c) B Lymphocytes adhered nonspecifically to a (PDAC4/SPS4)_{15.5} film, which is the background (i.e., interstitial) surface. Scale bars = 50 μ m.

Table 2. Quantification of the Different Cell-Attachment Scenarios as a Function of Film Deposition Conditions and Seeding Time^a

	HA-topped (built without NaCl; Figure 4a)	HA-topped (built with NaCl; Figure 4b)	HA-topped (built with NaCl; Figure 5a)	CHI-topped (built without NaCl; Figure 5b)
	cells seeded for 1 h		cells seeded for 2 h	
occupied array sites (%)	56.9	71.1	96.7	90.6
two cells sharing a site (%)	0.7	0.9	1.9	1.1
cells off array sites (%)	2.2	2.7	2.5	2.0

^a All films were assembled at pH 3.0. Total array occupancy increases with seeding time, but the number of cells off array sites is constant, indicating that off-array attachment is nonspecific.

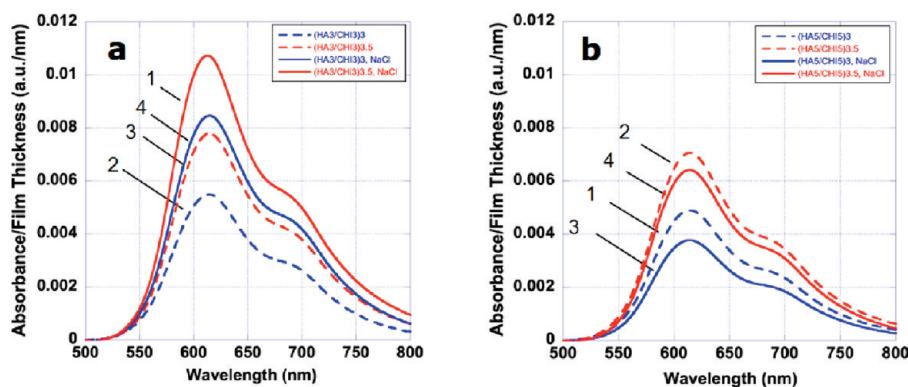


Figure 6. Alcian blue absorbance for (a) (HA3/CHI3) and (b) (HA5/CHI5) films normalized by film thickness. The numbers 1–4 correspond to films with the greatest to the least lymphocyte binding capability.

multilayer. The second test involved the use of soluble HA as an antagonist for cell binding (M_w , 1.58×10^6 g/mol, solution concentration, 200 mg/mL). B cells were seeded onto patterned HA or CHI-topped films built with and without 100 mM NaCl, respectively, and soluble HA was added to competitively bind with CD44 or CHI (see Supporting Information for array micrographs). The introduction of soluble HA caused a decrease in array occupancy for both the CHI- and HA-topped films. In the former case, the occupancy level dropped by 60%, whereas in the latter case, it dropped by about 12%. The higher drop in occupancy for the CHI-topped multilayer suggests a weaker binding interaction in this case. Consistent with this idea, it has been observed that when B cells adhered to multilayers are subjected to a flow of PBS solution over the surface, B cells attached to HA-topped films display a greater resistance to detachment in comparison to B cells attached to CHI-topped multilayers. These results are consistent with our previous finding that adding soluble HA to a B cell suspension prior to exposure to a patterned CHI/HA multilayer dramatically decreased cell binding due to saturation of the cell's CD44 receptors with soluble HA.⁴ These experiments combined strongly suggest that CD44–HA interactions are the dominant binding mode in all HA-containing films: even those assembled with CHI in the final deposition step.

Determination of Free HA Carboxylate and CHI Ammonium Groups. To indirectly explore changes in the amount of nonionically complexed, cell-accessible HA chain

segments presented under different assembly conditions, we used specific dyes known to bind to charged HA and CHI functional groups. Small molecule dyes have previously been shown to stain only free, nonpolymer paired ammonium or carboxylate groups and do not titrate electrostatically paired groups;³³ we assume the dyes used in this study act similarly. The free carboxylic acid groups of HA were stained with alcian blue, a tetracationic dye that has been used to probe polyanionic substances such as hyaluronic acid.^{34,35} Staining with rose bengal, an anionic dye, was used to evaluate the presence of the free ammonium groups of CHI. In both cases, we assume that the amount of dye uptake is determined primarily by the number of free, nonpolymer partnered anionic (HA case) or cationic (CHI case) charges.

Alcian blue staining results for multilayers prepared with pH 3.0 and 5.0 assembly conditions are shown in Figure 6a and b, respectively. The complementary rose bengal staining results are shown in Figure 7a and b.

As observed in these figures, all multilayer films were stained by both dyes, regardless of the final polymer deposited. This suggests that these are highly intermixed multilayers with the ionic functional groups of both polymers available at or near the surface (depending on multilayer swellability and diffusion times, dyes can penetrate and access free ionic functional groups deeper into the multilayer) and that no assembly conditions produced an outermost layer arrangement capable of blocking the uptake of an oppositely charged dye.³³

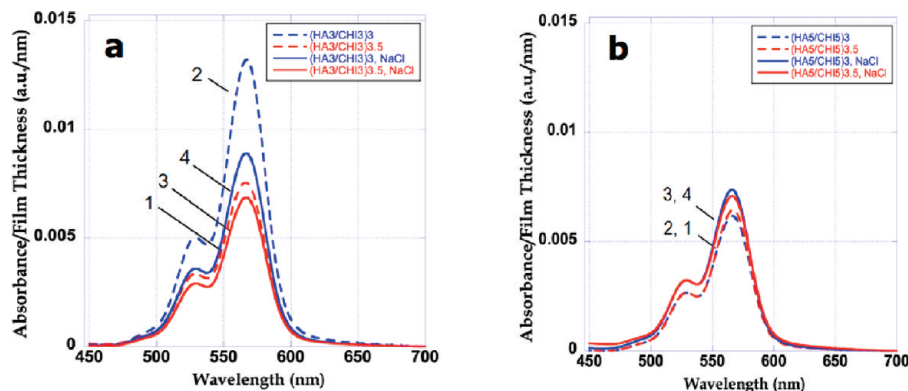


Figure 7. Rose bengal absorbance per film thickness for (a) (HA3/CHI3) and (b) (HA5/CHI5) films. The numbers 1–4 correspond to films with the greatest to the least lymphocyte binding capability.

Figure 6a shows that PEMs prepared at pH 3.0 with NaCl and regardless of final polymer deposited display the strongest alcian blue absorbance and thus have the most free HA chain segments. Preparing a film at pH 3.0 with NaCl increases the alcian blue absorbance value over a film prepared without salt. These trends were not observed under pH 5.0 deposition conditions (Figure 6b), where the two highest alcian blue absorbance values were found for HA-terminated films, regardless of salt condition, and preparing a film without NaCl increases its absorbance value over a film prepared with salt.

Rose bengal staining of free cationic charges is shown in Figure 7. These data revealed that CHI-terminated films assembled at pH 3.0 (labeled 2 and 4 in Figure 7a) have the largest amount of free cationic groups. In contrast, HA-terminated films exhibit lower amounts of free ammonium groups, as seen by the absorbance curves labeled 1 and 3 in Figure 7a. The addition of salt to the deposition solutions reduces the number of free cationic groups relative to the same multilayer prepared without salt (compare curves 2 and 4 and 1 and 3, Figure 7a). These trends were seen only under pH 3.0 deposition conditions; at assembly pH 5.0, the free ammonium group concentration is essentially insensitive to deposition conditions (final polymer deposited and salt).

Discussion

HA- and CHI-containing PEMs are interesting for a host of biological applications because of their well-established biocompatible and biodegradable properties.^{6,15,36–38} In the specific case of immune system engineering, a six-sugar sequence of HA is a natural ligand for the CD44 surface receptor found in many immune system cells.¹⁰ To take full advantage of this potentially powerful cell–polymer interaction, it is necessary to create molecular assemblies that present their critical binding functional groups in an optimal arrangement. To accomplish this goal, we examined how deposition conditions influence the molecular-level blending¹² of these two polymers during multilayer assembly. Three deposition variables were studied in depth: the presence of NaCl in the polymer solutions (0 or 100 mM), the pH of the polymer solutions (3.0 or 5.0), and the final polymer deposited (HA or CHI).

The two most efficient B cell attracting multilayer films were both assembled at pH 3.0. In one case, HA was the final deposited polymer and 100 mM NaCl was added to the deposition solutions. In the other case, CHI was the last deposited polymer and no NaCl was added to the deposition solutions. In the former case, the resultant multilayer film exhibited the highest concentration of free HA segments, as

revealed by alcian blue staining. If one accepts the hypothesis that B cell binding to HA/CHI multilayers is facilitated by a CD44 receptor interaction with chain segments from HA, then it would be expected that the multilayer presenting the highest concentration of free HA segments would be the most effective at binding B cells. However, the fact that the CHI-topped multilayer film assembled at pH 3.0 exhibited the largest amount of free cationic groups (and much lower alcian blue staining) suggests that the positively charged CHI chains in this case are also contributing to the high binding efficiency. Cationic charges may enhance cell binding because B cells have a negatively charged membrane. Hence, both HA–CD44 binding and electrostatic interactions can be in play with HA/CHI multilayers.

Suitable control experiments confirmed that HA is required for successful B cell attachment. In all cases examined (assembly pH 3.0 or 5.0, with and without salt), HA containing multilayers were found to exhibit the ability to adhere and immobilize B cells from culture solutions. In contrast, when HA was replaced in the multilayer with the structurally similar ALG, no B cell binding was observed. Indeed, the ALG/CHI multilayer films investigated in this study proved to be excellent B cell adhesion blocking multilayers. Similarly, multilayer films containing PDAC/SPS only exhibited a weak ability to bind B cells. In a separate study of the wet-state mechanical properties of these films, as determined by nanoindentation experiments, it has been determined that there is no strong correlation between film stiffness and B lymphocyte adhesion.³⁹

In further support of the idea that B cell binding is facilitated by HA segments, the introduction of soluble HA was found to promote the release of B cells previously attached to HA/CHI multilayers. The pronounced difference in the number of cells released from the most efficient cell binding HA- and CHI-topped multilayers (12 vs 60%, respectively) indicates that the adhesion between B cells and the CHI-topped multilayer is considerably less strong. This observation supports the notion that, in the CHI-topped case, electrostatic interactions between positively charged CHI chains and negatively charged cells are, in part, responsible for the high B cell binding efficiency of this multilayer system. Although electrostatic interactions can lead to a high cell binding efficiency, with fewer CD44 ligand sites available at the surface, the B cells are readily displaced from the multilayer by the receptor competitive HA chains in solution. Furthermore, we have observed that B cells adhered to HA-topped multilayers are much more resistant to detachment when subjected to an aggressive flow of PBS solution over the surface. Thus, if one seeks a high binding efficiency coupled with more strongly adherent cells, assembly conditions that

produce the highest level of free, surface accessible HA segments are the best option.

The ability to terminate a film in either HA or CHI and achieve similar binding efficiency may be of particular interest for some applications. If application requirements dictate a need for particular functional groups on the surface (carboxylates on HA, amines on CHI), then either HA or CHI may be used without impairing B-cell binding capability. In addition, the known antibacterial properties of CHI⁹ might be better exploited when CHI is the last deposited layer.

Finally, we note that while specific assembly conditions could be identified that promote a high level of B cell binding, a clear and direct correlation between the total amount of free HA segments (as revealed by alcian blue staining) and B cell binding was not uncovered. This reflects the fact that, as mentioned above, electrostatic interactions may also play a role, resulting in a complex interplay between cell binding and the number of available HA segments and positively charged CHI chains at or near the surface. In addition, how the HA binding ligands are presented at the surface (in loops and/or tails, for example), not the total quantity of HA, is far more important for efficient CD44 binding. Lower assembly pH and the addition of salt to the deposition solutions would be expected to favor a higher concentration of loops and tails.

Conclusions

Biopolymer multilayers comprised of hyaluronic acid and chitosan successfully immobilize nonadherent B lymphocytes. These films bind to B lymphocytes via a native CD44–hyaluronate interaction, ensuring their viability and function following attachment. We were able to maximize binding efficiency of the PEMs by systematically adjusting solution deposition variables such as ionic strength and pH. From all of the biopolymer multilayer systems studied, the greatest lymphocyte binding was found for the HA-terminated (HA3/CHI3)_{3.5} film deposited with 100 mM NaCl. Very similar binding levels were found for the CHI-terminated (HA3/CHI3)₃ film deposited without salt. Lymphocytes bind to photolithographically patterned HA/CHI film arrays, corroborating previous findings.

This work demonstrates two important conditions for successfully attaching B cells to HA-containing PEM films. First, HA is essential for CD44-mediated binding, as shown by the ALG controls and antagonistic binding by soluble HA. However, as the dye staining data show, the total amount of HA in a multilayer does not necessarily determine B cell binding capability. Second, HA deposition conditions that favor loops and tails, such as low pH and with added salt, can result in greater B cell attachment by making more CD44-binding ligands available. These two conditions emphasize that how HA is presented on a surface is the most important factor determining cell binding potential. We believe the ability to easily produce CD44-binding thin films with tunable binding affinity will find numerous applications in biosensing, biomaterials, and tissue and immune system engineering applications. Furthermore, the natural interaction between CD44 and HA could initiate cell signaling cascades and prompt behavior desirable for biosensing, an application that originally motivated this work.³

Acknowledgment. We thank Prof. Darrell Irvine (DMSE, Massachusetts Institute of Technology) for his laboratory support in the lymphocyte work and Dr. Ray Turner for useful discussions about the use of alcian blue dye. This work was supported primarily by the MRSEC Program of the National Science Foundation under Award No. DMR-0819762. This

material is based on work supported under a National Science Foundation Graduate Research Fellowship. F.C.V. gratefully acknowledges the Brazilian Government Agency CAPES, under Grant No. 1101-08-0, for financially supporting his stay at MIT during this work.

Supporting Information Available. HA/CHI film growth curves on (PDAC4/SPS4)_{15.5} prelayers, array micrographs of B cells for the soluble HA competitive binding tests, and schematics of the multilayer patterned array-B cell system. This material is available free of charge via the Internet at <http://pubs.acs.org>.

References and Notes

- (1) Kim, H.; Doh, J.; Irvine, D.; Cohen, R.; Hammond, P. *Biomacromolecules* **2004**, *5*, 822–827.
- (2) Kim, H.; Cohen, R.; Hammond, T.; Irvine, D. *Adv. Funct. Mater.* **2006**, *16*, 1313–1323.
- (3) Rider, T. H.; Petrovick, M. S.; Nargi, F. E.; Harper, J. D.; Schwoebel, E. D.; Mathews, R. H.; Blanchard, D. J.; Bortolin, L. T.; Young, A. M.; Chen, J.; Hollis, M. A. *Science* **2003**, *301*, 213–215.
- (4) Swiston, A. J.; Cheng, C.; Um, S. H.; Irvine, D. J.; Cohen, R. E.; Rubner, M. F. *Nano Lett.* **2008**, *8*, 4446–4453.
- (5) *Multilayer Thin Films: Sequential Assembly of Nanocomposite Materials*; Decher, G.; Schlenoff, J. B., Eds; Wiley-VCH: Weinheim, 2003.
- (6) Richert, L.; Lavalle, P.; Payan, E.; Shu, X. Z.; Prestwich, G. D.; Stoltz, J.-F.; Schaaf, P.; Voegel, J.-C.; Picart, C. *Langmuir* **2004**, *20*, 448–458.
- (7) Elbert, D. L.; Herbert, C. B.; Hubbell, J. A. *Langmuir* **1999**, *15*, 5355–5362.
- (8) Denuziere, A.; Ferrier, D.; Damour, O.; Domard, A. *Biomaterials* **1998**, *19*, 1275–1285.
- (9) Kumar, M. N. V. R.; Muzzarelli, R. A. A.; Muzzarelli, C.; Sashiwa, H.; Domb, A. J. *Chem. Rev.* **2004**, *104*, 6017–6084.
- (10) Underhill, C. J. *Cell Sci.* **1992**, *103*, 293–298.
- (11) Dubas, S. T.; Schlenoff, J. B. *Macromolecules* **1999**, *32*, 8153–8160.
- (12) Shiratori, S. S.; Rubner, M. F. *Macromolecules* **2000**, *33*, 4213–4219.
- (13) Hillberg, A. L.; Tabrizian, M. *Biomacromolecules* **2006**, *7*, 2742–2750.
- (14) Krol, S.; Nolte, M.; Diaspro, A.; Mazza, D.; Magrassi, R.; Gliozzi, A.; Fery, A. *Langmuir* **2005**, *21*, 705–709.
- (15) Thierry, B.; Winnik, F. M.; Merhi, Y.; Silver, J.; Tabrizian, M. *Biomacromolecules* **2003**, *4*, 1564–1571.
- (16) Croll, T. I.; O'Connor, A. J.; Stevens, G. W.; Cooper-White, J. J. *Biomacromolecules* **2006**, *7*, 1610–1622.
- (17) Schneider, A.; Richert, L.; Francius, G.; Voegel, J.-C.; Picart, C. *Biomed. Mater.* **2007**, *2*, S45–S51.
- (18) Chua, P.-H.; Neoh, K.-G.; Kang, E.-T.; Wang, W. *Biomaterials* **2008**, *29*, 1412–1421.
- (19) Berg, M. C.; Yang, S. Y.; Hammond, P. T.; Rubner, M. F. *Langmuir* **2004**, *20*, 1362–1368.
- (20) Richert, L.; Lavalle, P.; Vautier, D.; Senger, B.; Stoltz, J. F.; Schaaf, P.; Voegel, J. C.; Picart, C. *Biomacromolecules* **2002**, *3*, 1170–1178.
- (21) Mendelsohn, J. D.; Yang, S. Y.; Hiller, J. A.; Hochbaum, A. I.; Rubner, M. F. *Biomacromolecules* **2002**, *4*, 96–106.
- (22) Kidambi, S.; Udupa, N.; Schroeder, S. A.; Findlan, R.; Lee, I.; Chan, C. *Tissue Eng.* **2007**, *13*, 2105–2117.
- (23) Shaikh Mohammed, J.; DeCoster, M. A.; McShane, M. J. *Biomacromolecules* **2004**, *5*, 1745–1755.
- (24) Shaikh Mohammed, J.; DeCoster, M. A.; McShane, M. J. *Langmuir* **2006**, *22*, 2738–2746.
- (25) Denuziere, A.; Ferrier, D.; Domard, A. *Carbohydr. Polym.* **1996**, *29*, 317–323.
- (26) Rinaudo, M.; Pavlov, G.; Desbrières, J. *Polymer* **1999**, *40*, 7029–7032.
- (27) Lapčák, L., Jr.; Lapčák, L.; De Smedt, S.; Demeester, J.; Chabreček, P. Hyaluronan: Preparation, Structure, Properties, and Applications. *Chem. Rev.* **1998**, *98*, 2663–2684.
- (28) Cleland, R. L.; Wang, J. L.; Detweiler, D. M. *Macromolecules* **1982**, *15*, 386–395.
- (29) Porcel, C.; Lavalle, P.; Ball, V.; Decher, G.; Senger, B.; Voegel, J.-C.; Schaaf, P. *Langmuir* **2006**, *22*, 4376–4383.
- (30) Porcel, C.; Lavalle, P.; Decher, G.; Senger, B.; Voegel, J. C.; Schaaf, P. *Langmuir* **2007**, *23*, 1898–1904.
- (31) Richert, L.; Engler, A. J.; Discher, D. E.; Picart, C. *Biomacromolecules* **2004**, *5*, 1908–1916.
- (32) Schlenoff, J. B.; Dubas, S. T. *Macromolecules* **2001**, *34*, 592–598.

- (33) Yoo, D.; Shiratori, S. S.; Rubner, M. F. *Macromolecules* **1998**, *31*, 4309–4318.
- (34) Whiteman, P. *Biochem. J.* **1973**, *131*, 343–350.
- (35) Fagnola, M.; Pagani, M. P.; Maffioletti, S.; Tavazzi, S.; Papagni, A. *Contact Lens Anterior Eye* **2009**, *32*, 108–112.
- (36) Etienne, O.; Schneider, A.; Taddei, C.; Richert, L.; Schaaf, P.; Voegel, J.-C.; Egles, C.; Picart, C. *Biomacromolecules* **2005**, *6*, 726–733.
- (37) Picart, C.; Schneider, A.; Etienne, O.; Mutterer, J.; Schaaf, P.; Egles, C.; Jessel, N.; Voegel, J. C. *Adv. Funct. Mater.* **2005**, *15*, 1771–1780.
- (38) Schneider, A.; Vodouhe, C.; Richert, L.; Francius, G.; Le Guen, E.; Schaaf, P.; Voegel, J.-C.; Frisch, B.; Picart, C. *Biomacromolecules* **2007**, *8*, 139–145.
- (39) Unpublished results from a separate study in collaboration with Prof. Krystyn Van Vliet and Adam S. Zeiger, Department of Materials Science and Engineering, MIT, 2010.

BM100570R